Highly Emissive Colloidal CdSe/CdS Heterostructures of Mixed Dimensionality

ARTICLE *in* NANO LETTERS · DECEMBER 2003

Impact Factor: 13.59 · DOI: 10.1021/nl034815s

NANO LETTERS

xxxx
Vol. 0, No. 0
A−E

Highly Emissive Colloidal CdSe/CdS Heterostructures of Mixed Dimensionality

Dmitri V. Talapin,*,† Robert Koeppe,‡ Stephan Götzinger,§ Andreas Kornowski,† John M. Lupton,‡ Andrey L. Rogach,‡ Oliver Benson,§ Jochen Feldmann,‡ and Horst Weller*,†

Institute of Physical Chemistry, University of Hamburg, Bundesstr. 45, 20146 Hamburg, Germany, Photonics and Optoelectronics Group, Physics Department and CeNS, University of Munich, Amalienstr. 54, 80799 München, Germany, and Humboldt-Universität zu Berlin, Institut für Physik, Hausvogteiplatz 5-7, 10117 Berlin, Germany

Received September 23, 2003; Revised Manuscript Received October 12, 2003

ABSTRACT

We demonstrate that efficient shape control may be achieved in the shell of colloidally grown semiconductor nanocrystals (independent of the core), allowing the combination of a 0-D spherical CdSe core with a 1-D rodlike CdS shell. Besides exhibiting linearly polarized emission with a room-temperature quantum efficiency above 70%, these mixed-dimensionality colloidal heterostructures display large, length-dependent Stokes shifts as well as giant extinction coefficients approaching $10^7 cm^{-1} M^{-1}$.

Recent progress in the colloidal synthesis of semiconductor nanocrystals[1−3] has triggered a burst of research toward applications in biolabeling,[4] photonics,[5] and optoelectronics[6] as well as leading to a deeper understanding of the underlying physics in the quantum confinement regime.[2,7] Growing an epitaxial shell of a wide band gap semiconductor around a nanocrystal core, commonly CdSe, significantly improves the stability to photooxidation and increases the photoluminescence quantum yield (PLQY) to values up to 80%.[8,9] Nanocrystal shape control allows further engineering of properties such as PL polarization and alignability.[1,10]

The colloidal synthesis of semiconductor nanocrystals involves the formation of a desired crystalline phase in the presence of surfactant molecules adsorbing to the crystal surface. The specific adsorption of surfactants to the individual crystallographic planes alters the relative growth rates of different facets, providing a way of controlling the nanocrystal shape.[10,11] In this letter, we demonstrate for the first time the possibility of selective nucleation and epitaxial growth of another material on a particular crystallographic facet, allowing shape control of colloidal semiconductor heterostructures of mixed dimensionality. This provides an approach to tuning the crystal field experienced by the nanocrystals, which controls the electronic structure.[12−14]

Figure 1 shows transmission electron microscope (TEM) images of the rodlike CdSe/CdS core−shell particles (b, c, e−g) grown from the spherical CdSe nanocrystals (a, d), which display a high degree of crystallinity and monodispersity. At the first stage of the synthesis, CdSe core nanocrystals with narrow (4−7% std dev) size distributions (Figure 1a) were synthesized in the coordinating solvent mixture of hexadecylamine (HDA), tri-*n*-octylphosphine oxide (TOPO), and tri-*n*-octylphosphine (TOP) using dimethylcadmium and tri-*n*-phosphine selenide (TOPSe) as cadmium and selenium precursors, correspondingly.[15] CdS shells were grown on the CdSe cores by slowly adding a solution of cadmium and sulfur precursors to a diluted dispersion of CdSe cores in the HDA−TOPO−TOP mixture. In a typical preparation, 1.4 g of the crude solution containing ∼16 mg of CdSe nanocrystals was mixed with 7.5 g of HDA and 1.5 g TOPO, the reaction mixture was heated to 130 °C, and the desired amount of Cd/S stock solution was added dropwise (∼1 drop/s). The stock solution for growing the CdS rodlike shell was prepared by mixing 0.06 mL of dimethylcadmium, 0.475 mL of bis-trimethylsilylsulfide, and 5 mL of TOP. After adding the stock solution, the reaction mixture was cooled to 90 °C and was left for 1 h under stirring. Finally, the solution was cooled to room temperature, and highly luminescent CdSe/CdS nanorods were isolated by filtration or centrifugation

* Corresponding authors. D.V.T. E-mail: talapin@chemie.uni-hamburg.de. H.W. E-mail: weller@chemie.uni-hamburg.de. Fax: +49-40-42838-3452. Home page: http://www.chemie.uni-hamburg.de/pc/Weller/.
† University of Hamburg.
‡ University of Munich.
§ Humboldt-Universität zu Berlin.

10.1021/nl034815s CCC: $25.00
Published on Web 00/00/0000

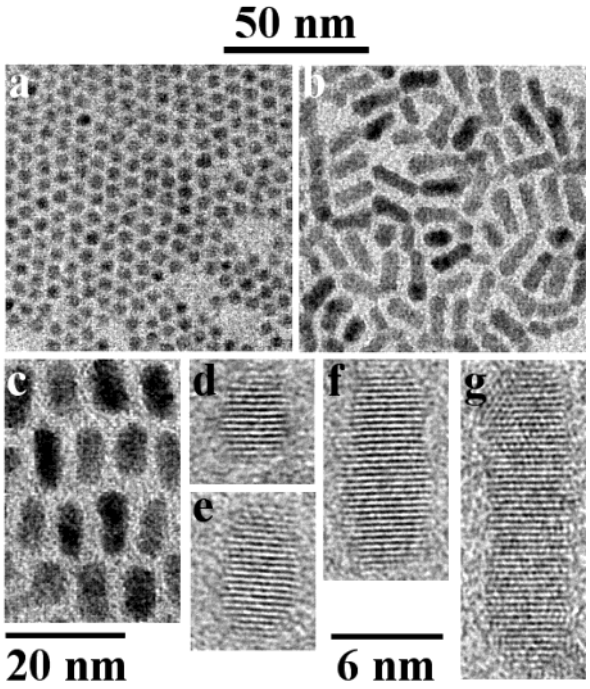

Figure 1. Overview TEM images of (a) spherical CdSe nanocrystals used as seeds for the growth of (b) CdSe/CdS nanorods. (c) CdSe/CdS nanorods aligned on a TEM grid upon evaporating the solvent. High-resolution TEM images of (d) spherical CdSe nanocrystals and (e−g) CdSe/CdS nanorods with different aspect ratios prepared by the asymmetric epitaxial growth of the CdS shell on spherical CdSe seeds. The diameter of the rods is comparable to the diameter of the spherical seeds.

after precipitating them with methanol. The nanorods are easily dispersible in chloroform or hexane.

The relatively low temperature used for growing the CdS shell prevented the alloying of the core and shell materials.[9] If the molar ratio of cadmium and sulfur precursors was in the range from ∼1:1 to 1:1.6, then spherical CdSe/CdS nanocrystals with a well-controlled shell thickness were formed.[16] In the presence of an excess of the sulfur precursor (Cd/S = 1:3−1:5), an asymmetric growth of the CdS shell leading to rodlike nanocrystals with an aspect ratio of up to ∼ 5:1 took place. Using CdSe cores of different sizes, the diameter of the nanorods can be varied from ∼3 to 6 nm. Their length can be easily tuned by changing the amount of shell precursors added (Figure 1e−g). The nanorods grown at relatively low reaction temperatures (120−130 °C) had the same diameter as the initial cores because of purely asymmetric shell growth, whereas at higher temperatures (140−180 °C) the growth along the *c* axis was accompanied by an increase in particle diameter. In contrast, nanocrystals prepared at 280 °C have a spherical shape due to the isotropic growth of the CdS shell (Figure S1 in Supporting Information).

The evolution of the powder X-ray diffraction patterns during the transformation of spherical CdSe particles into CdSe/CdS nanorods (Figure 2a) shows that the wurtzite phase in which the CdSe cores grow carries through to the CdS shell with no or few lattice dislocations. The attenuation of the (102) and (103) reflexes in powder X-ray diffraction patterns of CdSe/CdS nanorods can be explained by the

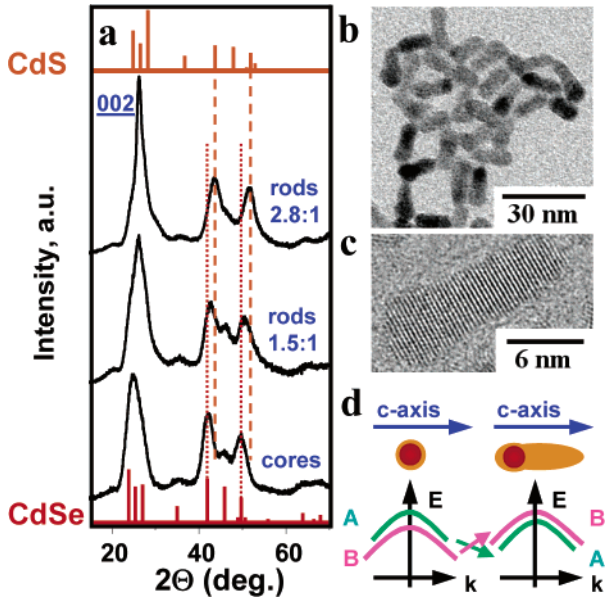

Figure 2. (a) Powder X-ray (Cu Kα radiation) diffraction patterns of the spherical CdSe cores and two samples of CdSe/CdS nanorods (aspect ratios 1.5:1 and 2.8:1) showing the crystallinity of all samples as well as the evolution from the pure hexagonal phase of CdSe to a system dominated by the hexagonal phase of CdS. The higher intensity and smaller width of the (002) reflection show that the long axis of the CdSe/CdS nanorods is the *c* axis of a wurtzite structure. The CdS reference is given in orange, and the CdSe reference, in red. (b) TEM image of CdSe/CdS nanorods showing the contrast change toward one end of the rods, which indicates that the cores are located at an asymmetric position inside the rods. (c) High-resolution TEM image of a CdSe/CdS nanorod with an asymmetric structure comprising a CdSe core uniformly covered with thin CdS shell and fused onto a CdS rod. (d) Valence-band scheme of a dot and a rod with the crossover between A and B bands induced by the crystal field along the *c* axis.

presence of stacking faults along the (002) direction.[2,10] The preferential growth of the CdS shell occurs along the *c* axis of the wurtzite structure while maintaining the diameter of the core.

We propose a microscopic mechanism for the asymmetric shell growth based on the intrinsic differences of the facets of hexagonal CdSe and CdS nanocrystals. A hexagonal-phase CdSe or CdS nanocrystal is terminated mainly by {100}, {001}, and {00$\bar{1}$} facets.[17] There are two factors contributing to the directed growth of the CdS shell. First, the mismatch between the lattice constants for hexagonal CdSe and CdS phases is larger along the *c* axis (001) (∼4.2%) than in the perpendicular (100) direction (∼3.8%), and the epitaxial growth of CdS on the {100} CdSe nanocrystal facet occurs with larger interfacial strain than on the {001} or {00$\bar{1}$} facets. Second, cadmium atoms on {100} and {001} facets each have only one dangling bond, but cadmium atoms on the {00$\bar{1}$} facet form three dangling bonds; therefore, this surface area is considered to be the chemically most active one.[18] Furthermore, the difference in the reactivity of the crystalline facets can be increased by the specific adsorption of a surfactant. A large excess of the sulfur precursor in the synthesis was found to be necessary for the asymmetric growth of a CdS shell on spherical CdSe cores. The sulfur precursor interacts preferentially with the growth-active

cadmium sites on the $\{00\bar{1}\}$ facet, resulting in the asymmetric nucleation of the CdS phase on the surface of the CdSe cores. The presence of hexadecylamine in the stabilizing mixture promotes further growth of the CdS shell along the *c* axis, as was observed for pure CdS nanocrystals.[19] The possibility of asymmetric nucleation and the preferential growth of the $\{00\bar{1}\}$ facet of the CdS shell are in agreement with the TEM measurements that show a darker region at one end of some nanorods (Figure 2b), which we attribute to the core. This suggests an asymmetric structure with a CdSe core covered by a very thin CdS shell fused onto one end of a CdS rod (Figure 2c).

The transition from the solely anisotropic growth of the CdS shell at low temperatures (120 °C) to isotropic growth at 280 °C can be explained if we consider both thermodynamic and kinetic factors affecting the shell growth. The difference in interfacial strain energy for the CdS shell growing on the different facets of the CdSe core results in favorable growth of the CdS shell along the (001) axis. However, at high temperature this energetic difference may approach the value of *kT*, resulting in a transition from anisotropic to isotropic growth of the CdS shell. The proposed kinetic model is based on the higher reactivity of the $\{00\bar{1}\}$ facet of CdSe seeds. The observed regimes of temperature-dependent shell growth can be determined by a transition from reaction kinetics-limited (anisotropic) growth at low temperatures to diffusion-limited (isotropic) shell growth at higher temperatures. Such a transition is expected to occur as the reaction rate increases more strongly with temperature than the rate of diffusion.

In CdSe/CdS nanocrystals, the electron is delocalized through the entire system as its effective mass, and the small conduction band offset of 0.2 eV is not sufficient to confine the electron to the CdSe core.[8,9] In contrast, the hole is more strongly confined to the spherical CdSe core because of its high effective mass and the large valence band offset of 0.55 eV.[8,9] In our asymmetric nanorods, we therefore expect a very different level of confinement of electrons and holes. The hole maintains 0-D character, whereas the electron gains 1-D character because of delocalization into the 1-D rodlike shell. The nanocrystals thus offer mixed dimensionality for electrons and holes.

Optical absorption spectra of CdSe/CdS nanorods dispersed in chloroform shown in Figure 3a display well-resolved electronic transitions that are slightly red-shifted with respect to those observed in the CdSe cores as well as a huge contribution from the CdS shell at wavelengths below 500 nm. The molar extinction coefficient[20] of nanorods with an aspect ratio of 4:1 reaches very high values of $\sim 10^7$ mol^{-1} cm^{-1} at 340 nm.

For excitation wavelengths above 450 nm, the absorption is traced very closely by the PL excitation spectrum, which is also shown in Figure 3a. Because photons with wavelengths below 500 nm are absorbed mainly in the CdS shell, this implies a very efficient capture of charge carriers in the core with virtually no loss to surface states. Time-resolved PL measurements carried out under excitation by a frequency-doubled fs Ti:sapphire laser and detection through either a

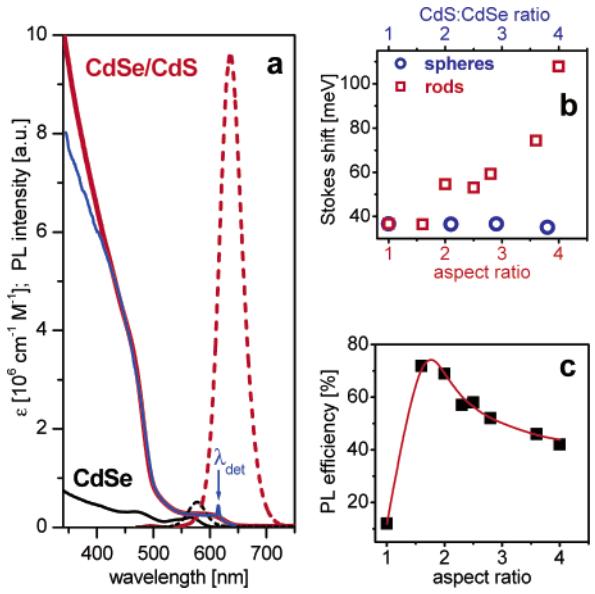

Figure 3. (a) Molar extinction coefficient ϵ for 4-nm CdSe cores (solid black line) and 17 nm × 4.5 nm CdSe/CdS nanorods (solid red line) dispersed in chloroform. The PL excitation spectrum of nanorods detected at an emission wavelength of 615 nm (solid blue line) closely traces the extinction coefficient, indicating efficient carrier capture in the core. The black and red dashed lines show PL spectra measured under excitation at 450 nm for CdSe cores and CdSe/CdS nanorods, respectively, normalized to the particle concentration. (b) Evolution of the global Stokes shift for CdSe/CdS nanorods with different aspect ratios. For comparison, we measured the global Stokes shifts of spherical core−shell CdSe/CdS nanocrystals upon increasing thickness of the CdS shell. CdSe/CdS nanorods and nanospheres can be compared by quoting the CdS/CdSe molar ratio (top axis). (c) Room-temperature PL quantum yield of CdSe cores and CdSe/CdS nanorods in chloroform vs their aspect ratio.

streak camera system or a time-correlated single-photon counting setup indicate that this capture process is completed in less than 5 ps, thereby enabling very high PL quantum yields. A steady slowing of the fluorescence decay observed with increasing aspect ratio suggests a reduction in the radiative decay rate due to a decrease in the oscillator strength per unit volume resulting from reduced electron−hole wave function overlap. This in turn implies a substantial delocalization of at least one of the carriers from the core into the shell. Additionally, the length of the CdS component appears to affect the level of confinement of the excited state because both PL and absorption spectra are found to shift to longer wavelengths with increasing aspect ratio.

The lowest excited state of wurtzite spherical nanocrystals is generally an A-type exciton, which is optically forbidden along the *c* axis, whereas emission occurs from a higher B-type state with a transition dipole moment orthogonal to the *c* axis of the wurtzite structure.[21] A nonspherical shape can lead to a swapping of the two states as sketched in Figure 2d, with a strongly allowed dipole resulting in the direction of growth (*c* axis) due to the perturbation induced by the crystal field.[12−14] Surprisingly, we find that the crystal field induced by a CdS epitaxial surface layer can have the same effect in heterogeneous nanoparticles. Evidence that the control of nanocrystal shell shape modifies the core electronic

properties comes from the evolution of the global Stokes shift with increasing shell thickness shown in Figure 3b. Whereas the Stokes shift of spherical core−shell nanocrystals is almost independent of CdS shell thickness, a continuous increase is observed for rods with increasing aspect ratio. Such a shape-dependent Stokes shift was predicted by Efros and Rodina[14] because of a swap-over of A and B valence bands. We observe a much larger Stokes shift for our heterogeneous nanorods than has previously been reported for pure CdSe rods[13] of the same aspect ratio. The larger Stokes shift in heterogeneous compared to homogeneous rods is most likely the result of a larger crystal field[14] required for moving the valence bands with respect to each other. In the case of heterogeneous rods, the lattice mismatch between core and shell will provide a further source of strain, thereby enhancing the hole-level perturbation.

The formation of an elongated CdS epitaxial shell on spherical CdSe cores results in a considerable increase of PLQY as well as photostability due to the effective passivation of CdSe surface states, which are involved in trapping and nonradiative recombination in bare CdSe nanocrystals. The absolute value of the room-temperature PLQY measured as described in ref 16 reaches 70−75% for CdSe/CdS nanorods with an aspect ratio of 1.6−2 and is still as high as 40−45% for rods with an aspect ratio of 4:1 (Figure 3c). The fact that the quantum yields are so high although electron penetration into the shell is expected to occur provides evidence that hole trapping at the nanoparticle surface is the luminescence-limiting process rather than the trapping of both carrier species. Asymmetric nanocrystals of mixed dimensionalities for electron and hole confinement therefore allow fundamental insight into the fluorescence-limiting processes in colloidal nanocrystals.

We also observed a strong increase in PLQY for CdSe/CdS nanorods with a diameter very similar to that of the original CdSe seeds. This implies that the (100) facets of the CdSe core were not covered by any CdS shell. We can propose two possible explanations for the PLQY increase in this case. First, some reconstruction and annealing processes on the (100) facets may occur upon growing the CdS shell at low temperatures, thereby reducing the number of luminescence-quenching surface defects. Indications for such a process come from the recent observation that CdSe nanocrystals can exhibit very high PL quantum efficiencies even without coating with inorganic shells.[22] Second, one can assume that the surface dangling bonds on the polar {001} and {00$\bar{1}$} facets of the CdSe nanocrystal have a major impact on the nonradiative recombination processes, and their selective passivation with an epitaxial inorganic shell can therefore provide a substantial increase in the overall PLQY.

The emission band of the heterogeneous CdSe/CdS nanorods is always observed in the spectral region where only the CdSe core can reabsorb the emitted light. The extinction coefficients in this spectral region are small in comparison to those of the CdS rodlike antenna (Figure 3a). This means that reabsorption effects in solutions and films of CdSe/CdS nanorods will be considerably smaller than reabsorption effects observed for CdSe nanorods or CdSe/ZnS core−shells

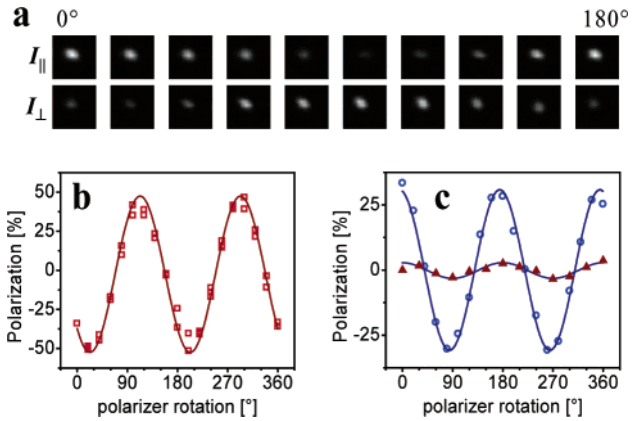

Figure 4. (a) Series of PL images of a single CdSe/CdS nanorod recorded simultaneously in two perpendicular polarization directions. The detection angle was changed stepwise from 0 (left side) to 180° (right side). (b) PL intensity ratio $(I_{\parallel} - I_{\perp})/(I_{\parallel} + I_{\perp})$ of a single CdSe/CdS nanorod with an aspect ratio of 1:4 (red open squares) as a function of polarizer angle. (c) PL intensity ratio $(I_{\parallel} - I_{\perp})/(I_{\parallel} + I_{\perp})$ of a CdSe/CdS nanorods ensemble (aspect ratio 2.8:1) in a stretched polymer matrix (blue circles) and of CdSe spherical cores (black triangles) as a function of polarizer angle. The solid lines are $\cos^2$ fits showing a high degree of polarization for CdSe/CdS nanorods in both cases.

prepared by growing ZnS shells around CdSe nanorods.[23] The high fluorescence yields in combination with the large Stokes shift and reduced reabsorption effects make CdSe/CdS core−shell rods particularly useful for solid-state luminescence applications such as light-emitting diodes and lasers.

Single-particle spectroscopy on CdSe/CdS heterogeneous nanorods was carried out at room and at low temperatures in an epifluorescence microscope similarly to previous descriptions.[24] The PL light from single rods dispersed in a PMMA matrix was sent through a rotating halfwave plate, split by a Wollaston prism into two perpendicularly polarized beams, and then focused onto a highly sensitive CCD camera. In this way, two perdendicular polarizations could be observed simultaneously. Single-particle spectroscopy performed on CdSe/CdS nanorods revealed luminescence intermittency (blinking) similar to that previously reported for spherical CdSe/ZnS nanocrystals[24] as well as spectral diffusion at cryogenic temperatures, indicating that a single nanorod is observed at a time.[25] Single-particle spectroscopy reveals the linear polarization of the emission of CdSe/CdS nanorods with a polarization factor of up to 75% (i.e., $PL_H/PL_V = 5:1$) at room temperature. Figure 4a shows a series of luminescence images of a single CdSe/CdS nanorod simultaneously recorded in two perpendicular polarization directions. The detection angle was changed stepwise from 0 to 180° through a rotating polarizing beam splitter. Integrated PL intensities from a single CdSe/CdS nanorod exhibit the expected $\cos^2$ intensity dependence on angle (Figure 4b). Because the orientation of rods on the substrate in single-particle measurements is unknown, we also examined oriented ensembles of the rods. By dispersing rods in a free-standing polymer matrix and subsequently stretching the film to up to 5 times the original length, the rods are partially oriented similarly to those shown in Figure 1c. In all cases,

the PL as well as the absorption was found to be polarized parallel to the direction of stretching and thus parallel to the *c* axis of the rod. Figure 4c shows the PL intensity dependence for a nanorod ensemble in a stretched polymer matrix on polarizer angle. Time-resolved PL measurements (not shown) demonstrated that the polarization anisotropy in stretched films remains constant over at least 8 ns, suggesting that the effect of the crystal field on polarization is static. To confirm that the polarization of the oriented ensembles arises from the rods and not from the ordered dielectric environment, we also examined the polarization of spherical cores and core/shell particles in stretched films. In this case, the polarization effects were about 1 order of magnitude lower than for CdSe/CdS nanorods.

The simultaneous control of nanocrystal size and shape together with the possibility of growing heterostructures on certain nanocrystal facets opens up novel routes to the colloidal synthesis of more sophisticated heterostructures as building blocks for optoelectronics and nanoelectronics. The heterogeneous mixed-dimensionality quantum rods introduced here are a first step toward the colloidal synthesis of nanomaterials allowing different confinement regimes for electrons and holes. They also provide a direction toward colloidally grown heterostructures where CdSe "seeds" can be connected by CdS "bridges".[26] The interaction between these seeds can be studied in a well-defined system, which will be of use for future nanoelectronic applications. We anticipate that the superior optical properties of mixed-dimensionality heterogeneous nanocrystals in combination with straightforward synthetic methods will secure for these materials an important role in the entire palette of applications of colloidal nanocrystals.

Acknowledgment. We thank Sylvia Bartholdi-Nawrath for assistance with TEM and HRTEM investigations, Josef Müller, Felix Müller, Andrea Mazzei, and Florian Saas for help with the single-particle spectroscopy measurements, and Anna Rodina for helpful discussions. This work was supported by the BMBF, Philips and by the Deutsche Forschungsgemeinschaft through SFB 508, SFB 486, the "Schwerpunkt Photonische Kristalle", and the Gottfried-Wilhelm Leibniz Award.

Supporting Information Available: High-resolution TEM images of CdSe and CdSe/CdS nanocrystals synthesized at different temperatures and used for CdS shell growth. This material is available free of charge via the Internet at http://pubs.acs.org.

References

(1) Scher, E. C.; Manna, L.; Alivisatos, A. P. *Philos. Trans. R. Soc. London, Ser. A* **2003**, *361*, 241.
(2) Murray, C. B.; Kagan, C. R.; Bawendi, M. G. *Annu. Rev. Mater. Sci.* **2000**, *30*, 545.
(3) Rogach, A. L.; Talapin, D. V.; Shevchenko, E. V.; Kornowski, A.; Haase, M.; Weller, H. *Adv. Funct. Mater.* **2002**, *12*, 653.
(4) Bruchez, M. P.; Moronne, M.; Gin, P.; Weiss, S.; Alivisatos, A. P. *Science* **1998**, *281*, 2013.
(5) Norris, D. J.; Vlasov, Yu. A. *Adv. Mater.* **2001**, *6*, 371.
(6) Coe, S.; Woo, W.-K.; Bawendi, M.; Bulovic, V. *Nature* **2002**, *420*, 800.
(7) Alivisatos, A. P. *Science* **1996**, *271*, 933.
(8) Dabbousi, B. O.; Rodriguez-Viejo, J.; Mikulec, F. V.; Heine, J. R.; Mattoussi, H.; Ober, R.; Jensen, K. F.; Bawendi, M. G. *J. Phys. Chem. B* **1997**, *101*, 9463.
(9) Peng, X.; Schlamp, M. C.; Kadavanich, A.; Alivisatos, A. P. *J. Am. Chem. Soc.* **1997**, *119*, 7019.
(10) Peng, X.; Manna, L.; Yang, W. D.; Wickham, J.; Scher, E.; Kadavanich, A.; Alivisatos, A. P. *Nature* **2000**, *404*, 59.
(11) Manna, L.; Milliron, D. J.; Meisel, A..; Scher, E. C.; Alivisatos A. P. *Nature Materials* **2003**, *2*, 382.
(12) Hu, J.; Li, L.-s.; Yang, W.; Manna, L.; Wang, L.-w.; Alivisatos, A. P. *Science* **2001**, *292*, 2060.
(13) Wang, X.-J.; Zhang, J.-Y.; Nazzal, A.; Darragh, M.; Xiao, M. *Appl. Phys. Lett.* **2002**, *81*, 4829.
(14) Rodina, A. V.; Efros, Al. L. *Phys. Rev. B* **1993**, *47*, 10005. Efros, Al. L. *Phys. Rev. B* **1992**, *46*, 7448.
(15) Talapin, D. V.; Rogach, A. L.; Kornowski, A.; Haase, M.; Weller, H. *Nano Lett.* **2001**, *1*, 207.
(16) Mekis, I.; Talapin, D. V.; Kornowski, A.; Haase, M.; Weller, H. *J. Phys. Chem. B* **2003**, *107*, 7454.
(17) Shiang, J. J.; Kadavanich, A. V.; Grubbs, R. K.; Alivisatos A. P. *J. Phys. Chem.* **1995**, *99*, 17417.
(18) Peng, Z. A.; Peng, X. *J. Am. Chem. Soc.* **2001**, *123*, 1389.
(19) Jun, Y.-W.; Lee, S.-M.; Kang, N.-J.; Cheon, J. *J. Am. Chem. Soc.* **2001**, *123*, 5150.
(20) The values of molar extinction coefficients of CdSe/CdS nanorods were determined as follows. First, a careful analysis of TEM images of both as-prepared and size-selected fractions of CdSe/CdS nanorods showed the absence of nucleation of new CdS nanocrystals upon growing the CdS shell if the molar ratio of Cd and S precursors was 1:3. This implies that the concentration of particles in the reaction mixture remains constant during the shell growth and is equal to the initial concentration of CdSe cores. This concentration can be easily estimated because the molar extinction coefficients of CdSe nanocrystals are known (Yu, W. W.; Qu, L.; Guo, W.; Peng, X. *Chem. Mater.* **2003**, *15*, 2854). Consequently, we measured the evolution of the absorption spectra of CdSe/CdS nanorods and calculated their molar extinction coefficients using the estimated concentration of nanocrystals and optical densities of crude solutions.
(21) Nirmal, M.; Norris, D. J.; Kuno, M.; Bawendi, M. G.; Efros, Al. L.; Rosen, M. *Phys. Rev. Lett.* **1995**, *75*, 3728.
(22) Qu, L.; Peng, X. *J. Am. Chem. Soc.* **2002**, *124*, 2049.
(23) Manna, L.; Scher, E. C.; Li, L.-s.; Alivisatos, A. P. *J. Am. Chem. Soc.* **2002**, *124*, 7136. Mokari, T.; Banin, U. *Chem. Mater.* **2003**, *15*, 3955.
(24) Empedocles, S. A.; Norris, D. J.; Bawendi, M. G. *Phys. Rev. Lett.* **1996**, *77*, 3873.
(25) Neuhauser, R. G.; Shimizu, K. T.; Woo, W. K.; Empedocles, S. A.; Bawendi, M. G. *Phys. Rev. Lett.* **2000**, *85*, 3301.
(26) Wang, D.; Lieber, C. M. *Nat. Mater.* **2003**, *2*, 355.

NL034815S